J Nanostruct 16(2): 1955-1977, Spring 2026

RESEARCH PAPER

Formulation and Evaluation of Mesalazine Nanoemulsion for Rectal Administration

Russul Hameed*, Mowafaq M. Ghareeb

Department of Pharmaceutics, College of Pharmacy, University of Baghdad, Baghdad, Iraq

ARTICLE INFO

Article History:
Received 05 January 2026
Accepted 26 March 2026
Published 01 April 2026

Keywords:
Cremophor EL
Drug-excipients compatibility studies
Meslazine
Sodium butyrate
Ulcerative colitis

ABSTRACT

Mesalazine (MSZ) is an anti-inflammatory medication used to treat and maintain relief in mild to severe ulcerative colitis (UC) or Crohn's disease (CD). MSZ has been demonstrated to be an effective scavenger of reactive oxygen species, which significantly contribute to the pathogenesis of inflammatory bowel disease; to suppress natural killer cell activity; to inhibit antibody synthesis; to block cyclooxygenase and lipoxygenase pathways; and to impair neutrophil function. To prepare and stabilize mesalazine and increase intraluminal colonic concentrations. We determined the solubility of MSZ in different oils and surfactants. Based on the solubility results, we constructed a phase diagram and prepared a nanoemulsion with various oil types and ratios (vitamin E and imwitour 308).Smix using Cremophor EL and propylene glycol. After successful nanoemulsion preparation, an in vivo study was done. Nanoemulsion characteristics were evaluated by particle size (PS), polydispersity index (PDI), and drug content. In vitro drug release was compared by assessing changes resulting from variations in concentration and oil type. FTIR, PXRD, and TEM were used to further evaluate the optimum formula. the particle size of the formula ranged from 6nm to 574nm. The optimized formulation M11 and M20 was further evaluated for morphological characteristics. It revealed the presence of a spherical droplet. Fourier-transform infrared spectroscopy (FTIR) indicated no chemical interactions.

How to cite this article
Hameed R., Ghareeb M. Formulation and Evaluation of Mesalazine Nanoemulsion for Rectal Administration. J Nanostruct, 2026; 16(2):1955-1977. DOI: 10.22052/JNS.2026.02.044

INTRODUCTION

There are several ways to make poorly water-soluble medicines more soluble and more readily available to the body. Some of the primary ways to make drugs soluble include solid dispersion, co-solvency, micronization, nanonization, chemical modification, hydrotropy, complexation, micellar solubilization, pH manipulation, and others [1].

Several factors influence drug absorption and bioavailability. Factors such as dissolving rate, pH, delivery route, and first-pass metabolism influence drug efficiency. Medicines with low solubility and strong pharmacological effects often have reduced therapeutic efficiency due to their limited solubility and slow dissolution rates. As a result, higher doses may be required in clinical settings. Notably, this issue is significant since approximately 40% of

* *Corresponding Author Email: Rusul.atia2200@copharm.uobaghdad.edu.iq*

marketed drugs are classified as poorly soluble [2].

The BCS system categorizes drugs into four collections based on solubility and intestinal permeability, emphasizing their impact on drug absorption. Class I medications exhibit strong absorption, Class II pharmaceuticals possess poor solubility, Class III drugs have restricted permeability, and Class IV drugs are characterized by low absorption. [3,4].

Nanotechnology has emerged as a significant scientific advancement in the 21st century. This multidisciplinary field includes scientists synthesizing, manipulating, and applying materials with dimensions smaller than 100 nanometers. Nanoparticles provide considerable utility in diverse industries, such as environmental management. These fields include agriculture, food technology, biotechnology, biomedicine, and pharmaceuticals. Researchers use them in areas like wastewater treatment, environmental monitoring, as functional food additives, and as antimicrobial agents. [5].

Nanoemulsions are emulsions distinguished by droplet sizes of roughly 100 nm. A conventional nanoemulsion consists of oil, water, and an emulsifying agent. The use of an emulsifier is crucial for producing small droplets, since it lowers the interfacial tension between the oil and water phases of the emulsion. The emulsifier aids in the stabilization of nanoemulsions via repulsive electrostatic interactions and steric hindrance [6,7].

The formulation of nanoemulsion necessitates the incorporation of two immiscible liquids and an emulsifying agent. One of the immiscible liquids must be oleaginous, while the other is watery, constituting the scattered and continuous phases. The o/w and w/o [8,9].

A nanoemulsion is comprised of a core shell structure. The surfactants are added to the shell, and the core has nonpolar moieties in oil-in-water systems. Examples of the oil phases include triacylglycerols, essential oils, mineral oils, waxes, and oil-soluble vitamins. Properties of the oil phase (for example, viscosity, refractive index, density, or phase behavior) and interfacial tension influence how nanoemulsions will form, be stable, and function [10,11].

The non-ionic surfactant known as Cremophor EL, whose full name is polyoxyl 35 castor oil, stands out due to its diverse composition. It manifests as a light yellow viscous liquid. The estimated critical micelle concentration (CMC) is 0.02%. The hydrophilic-lipophilic balance (HLB) is between 12 and 14. Cremophor EL is produced by the reaction of castor oil with ethylene oxide at a molar ratio of 1:35. The pharmaceutical industry has devoted significant attention to its utilization because of its ability to solubilize, preserve, and encapsulate lipophilic bioactive substances [12,13].

Propylene glycol is a cosurfactant often used in topical formulations. Propylene glycol has both hydrophilic and hydrophobic groups, which may diminish the intermolecular attraction of water. Propylene glycol is a low-toxicity cosolvent [14].

One kind of short-chain fatty acid, sodium butyrate, is made from dietary fiber that is broken down by the microbes in the gut. Research has shown that butyrate is essential for controlling cell proliferation, apoptosis, and differentiation. This,

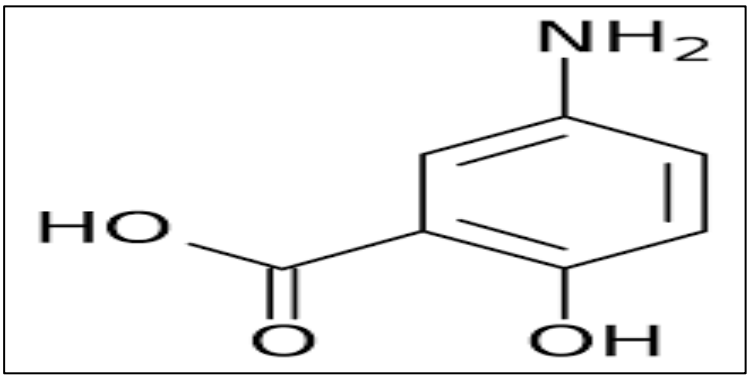

Fig.1. Chemical structure of mesalazine [21]

in turn, aids in guarding the integrity of the colonic mucosa in mice, which in turn helps them fight colitis [15-17].

Mesalazine (5-aminosalicylic acid) is the principal ingredient of sulfasalazine, a chemical extensively used in the management of ulcerative colitis and Crohn's disease. Administration is conducted either orally via different controlled-release formulations or rectally via suppositories, enemas, and foams [18].

Mesalazine (5-aminosalicylic acid) is the principal ingredient of sulfasalazine, a chemical extensively used in the management of ulcerative colitis and Crohn's disease. Administration is conducted either orally via different controlled-release formulations or rectally via suppositories, enemas, and foams [19]. Crystals ranging in color from white to pink are very weakly soluble in water and absorb 20-30% after oral dosing [20].

MATERIALS AND METHODS

Material

Mesalazine MSZ was obtained from Hyperchem, and the oils (Labrosol, Transculol, Cremophare, Oleic acid, Almond oil, Grape oil, Sesame oil, mm 948, Clove oil, Olive oil, Peppermint oil, Vitamin E, Jojoba oil, Frankincense oil, Labrafil oil, Labrafac oil, and Imwitor308) and other surfactants from Kathy.

Preformulation study

In addition to supporting formulation development, preformulation studies facilitate lead identification during drug discovery. A novel chemical entity must demonstrate optimal biopharmaceutical characteristics to be considered a viable therapeutic candidate. Potency and selectivity alone do not ensure drugability. Preformulation studies are essential for evaluating a compound's drugability and serve as a critical decision-making tool throughout both drug research and development phases.[22,23].

UV-wavelength (lambda max)

The lambda max(λmax) of Mesalazine was detected using two media, ethanol and Phosphate buffer pH 7.4. Accurately weighed mesalamine drug (10 mg) was dissolved in a 10 ml volumetric flask containing ethanol for the detection of ethanol λmax and in 10 ml of phosphate buffer, pH 7.4, for the detection of λmax in the phosphate buffer. The volume was increased to a level containing an adequate proportion of ethanol and phosphate buffer, pH 7.4. This resulted in a concentration of 100 µg/ml. Additionally, several aliquots were produced from the stock solution. The aliquots were analyzed by spectrophotometry (Shimadzu, UV-1800, Japan) [24].

Standard Curve Preparation

Mesalazine (MSZ) (10 mg) was precisely weighed and dissolved in a 100 ml volumetric flask containing phosphate buffer, pH 7.4, and ethanol individually. To get a 100 µg/ml concentration. The basic solution was used to create additional standard solutions of the medication. From the typical stock solution, several aliquot was measured using a UV-spectrophotometer (Shimadzu, UV-1800, Japan).

Solubility and stability Studies of MSZ

Solubility experiments use the standard shake-flask method. It is used to determine solubility values of MSZ in the different media, as shown in Table 1. Excess amounts of MSZ are placed into the plan tube containing 2 mL of other oils, surfactants, and co-surfactants. It will be tightly closed and placed on a water bath shaker. The drug solution was shaken for 48 hours. The supernatant was collected, and the drug content was determined spectrophotometrically. [25,26].

Differential scanning calorimetric (DSC)

Using a DSC-60 Plus equipment (Shimadzu, Japan), the thermodynamic properties of MSZ were examined. In aluminium pans, a sample weighing about 2 mg was heated from 30 to 400 °C at a rate of 10 °C/min while 50 mL/min of nitrogen was pumped through [27].

Construction of a phase diagram

One kind of short-chain fatty acid, sodium butyrate, is made from dietary fibre that is broken down by the microbes in the gut. Research has shown that butyrate is essential for controlling cell proliferation, apoptosis, and differentiation. This, in turn, aids in guarding the integrity of the colonic mucosa in mice, which in turn helps them fight colitis. Cremophor and propylene glycol were combined at fixed weight ratios (1:1, 1:2, 1:3, 2:1, and 3:1 w/w) to construct the phase diagram. Subsequently, Imwitor308308 and vitamin E were included in each S-mix at ambient temperature. The oil-to-S-mix ratio was modified from 9:1

to 8:2, 7:3, 6:4, 5:5, 4:6, 3:7, 2:8, and 1:9 (w/w) for each phase diagram. The oil-S mixtures were vigorously mixed while water was added drop by drop. Visual inspection at equilibrium revealed that the samples were completely see-through. The unacceptable NE appears to be optically opaque or gel-like due to the presence of phase separation. For each S-mix that produces NE, the ideal stability and droplet size were determined [28-30].

Preparation of NE formulations

Using a water titration technique, a variety of O/W NE formulations have been developed, as shown in Table 1. A high-speed homogenization technique prepares the nanoemulsions. In this the homogeneous solution composed of a surfactant and co-surfactant in a different S-mix ratio in weight ratio. After that oil add graduated (Imwitor308 308and vitamin E) indifferent composition and ratio as shown in Table1 that mixed for 7min, after formation of clear homogenous solution,50mg drug and 25 mg of sodium metabisulfate (antioxidant) was add to this solution with contuse stirring, water was added to that homogenous solution under constant homogenization. Then o/w emulsion was formed. The stirring was maintained to let the system reach equilibrium [31,32].

Thermodynamic stability studies

The generated NEs must exhibit sufficient stability to undergo thermodynamic stability assessments before optimisation as NE formulations successfully. All the NEs that did not exhibit phase separations underwent heating and cooling trials (H&C) after centrifugation (CEN) for 30 minutes at 4000 rpm. Three freeze-thaw cycles (F-T) were conducted on these formulations, with temperatures ranging from -20°C to 25°C. Physical characterization was performed on NE formulations after their successful completion of the preceding test [33,34].

Characterization of Mesalazine Nanoemulsion

Measurement of globule size and polydispersity Index

The Zetasizer, manufactured by Malvern Instruments Ltd in the United Kingdom, was used to determine the nanoemulsion particle

Table 1. Composition of Mesalazine nanoemulsion formulas.

Formula code	Cremophor: Propylene glycol	Type of oil	%of oil	%of Smix	%of deionized water
M1	1:1	vitamin E	25%	23%	47%
M2	1:1	vitamin E	40%	17.7%	42.5%
M3	1:2	vitamin E	25	42.5	32.5
M4	1:2	vitamin E	40	30	30
M5	1:3	vitamin E	25	25	50
M6	1:3	vitamin E	35	25	40
M7	3:1	vitamin E	25	30	45
M8	3:1	vitamin E	35	26	39
M9	1:1	VitE25%+Imwitor30875%	25	61.5	13.5
M10	1:1	VitE25%+imwitor30875%	40	50	10
M11	1:2	VitE25%+imwitor30875%	30	55	15
M12	1:2	VitE25%+imwitor30875%	40	45	5
M13	2:1	VitE25%+imwitor30875%	25	60	15
M14	2:1	VitE25%+imwitor30875%	35	50	15
M15	3:1	VitE25%+imwitor30875%	20	45	35
M16	3:1	VitE25%+imwitor30875%	30	40	30
M17	1:1	Imwitor308	25	45	30
M18	2:1	Imwitor308	30	47	23
M19	2:1	Imwitor308	35	43	22
M20	1:2	Imwitor308	30	50	20
M21	1:2	Imwitor308	35	47.5	17.5
M22	1:3	Imwitor308	20	35	45

size (PS) and polydispersity index (PDI) of all the formulations that were prepared. This dynamic light scattering apparatus measures the amount of light scattered by molecules as a function of time at a constant temperature of 25°C and a scattering angle of 90° [35,36].

Effect of the type of oil on the prepared nanoemulsion and globule size

Study the effect of the kind of oil used in the prepared nanoemulsion, as shown in the Table 1, the oils used (vitamin E oil, VitE25%+ Imwitor30875% and Imwitor308).

Effect of surfactant and co-surfactant ratio and percent of smix on prepared nanoemulsion and globule size

In preparation for the Construction of the phase diagram, we used different ratios of surfactant and cosurfactant. Cremophor and propylene glycol were mixed at constant weight ratios (1:1,1:2,1:3, and 2:1,3:1 w/w) to create the phase diagram. The percent and ratio of smix that affects the globule size of the prepared nanoemulsion.

Uniformity of drug composition

The MSZ percentage was quantified in each formula relative to a theoretical formulation quantity. One milliliter of the formula was diluted in an appropriate proportion of ethanol, then combined and sonicated for complete drug extraction. Lastly, the mixture was spun at 3000 rpm for 15 minutes to separate the excipients that had not dissolved. The resulting solution is diluted before being examined at its maximum absorption wavelength (λmax) using a UV-VIS spectrophotometer [37,38].

Transmittance percentage (%T)

The translucence of the prepared nanoemulsions was tested using a turbidity test. For each formula, 2 ml was taken, and its absorbance was measured with a UV/Vis spectrophotometer, using distilled water as the blank [34,39,40].

In vitro drug release investigation

The in vitro drug release study for all synthesized NS formulations was carried out using dissolution equipment type II with 800 ml of freshly prepared dissolution medium. A dialysis membrane (pore size 2.4 nm, molecular weight 8000–14000 kDa) was pre-treated by immersion in the medium for 24 hours before use. The phosphate buffer (pH 7.4) served as the release medium. The experiment was performed at 37±1°C with agitation at 50 rpm for 2 hours. The NS containing 50 mg of MSZ was placed inside the pre-treated membrane bag, which was securely closed at both ends to prevent leaks. At scheduled intervals (5, 10, 15, 20, 25, 30, 40, 50, 60, 75, 90, and 120 minutes), a 5 ml aliquot of the release medium was withdrawn and replaced with an equal volume of fresh medium to maintain sink conditions. The quantitative estimation of MSZ was done at its λ max of 330.5 nm.

The results obtained from the dissolution investigations were statistically verified with a similarity factor (f2). The f2 was used to evaluate comparable dissolution profiles (equation below).

$$f_2 = 50 \times log\ \{[1 + (1/\ n)\ \sum_{j=1}^{n} w|Rj - T|^2]^{0.5} \times 100\}$$

Here, the total number of times that dissolution has taken place is denoted by the letter (n). At time t, the dissolution values obtained from the reference sample and the test sample are represented by the symbols R and (T), respectively. It is regarded that the two dissolution profiles are comparable when the f2values fall within the range of fifty to one hundred. [41].

An analysis of the in vitro release kinetics of MTZ from the nanoemulsion formulation that was created was carried out in order to get an understanding of the behavior of drug release. A linear regression analysis was performed on these plots, and the correlation coefficient (R2) was calculated as a result [42,43].

Selection of Optimum MSZ Nanoemulsion Formulas

The selection of the optimal formula was conditional upon the results and data regarding transmittance percentage, Smix concentration, drug content, and in-vitro drug dissolution. The ideal nanoemulsion formulation is characterized by specific particle size and polydispersity index (PDI).

Fourier-transform infrared spectroscopy (FTIR)

It is essential to explore the purity and compatibility of MSZ with the components of nanoemulsion. Using a potassium bromide substance packed with the pure drug as a disc, the liquid sample is measured using a special cuvette. The scanned wavelength ranges from 400 to 4000 cm^{-1}, and the displayed spectra data is registered

for analysis and recording of any incompatibilities [44-47].

Powder X-ray Diffraction (PXRD)

crystalline composition of MSZ powder and MSZ formula was analyzed utilizing powder-X-ray diffraction (XRD - 6000 Shimadzu - Japan). Measurements were performed using a Cu Kα filter at a voltage setting of 40 kV and an electrical current of 30 mA. The scanning was conducted within a 2θ range of 2θ to 80θ [48].

Transmission Electron Microscopy (TEM)

Morphological characteristics. The surface morphology of MSZ-loaded nanoemulsion was determined using a transmission electron microscope (TEM) [49].

Stability Assessment on Storage

To assess the long-term physical and chemical stability, MSZ nanoemulsion samples were stored in sealed glass vials at ambient temperature (25°C) and under refrigeration (4°C) for 90 days. After storage, the formulations were analyzed for particle size, polydispersity index (PDI), drug content, and visually inspected for precipitation [8,13].

In-vivo Irritation Study

Experimental design

Mature rats, weighing between 200g and 210 g and being 8 to 9 weeks old, were utilized. Regulated temperature, humidity percentage, and light period were all typical in housing; they were rectally injected with MSZ nanoemulsion formula as shown in Table 2. The animals were divided into eight groups, each consisting of five animals. Colon samples were taken, preserved in buffered formalin, embedded in paraffin, and stained with hematoxylin and eosin for examination under a microscope [15].

Stability study

The stability of formulation was tested at two

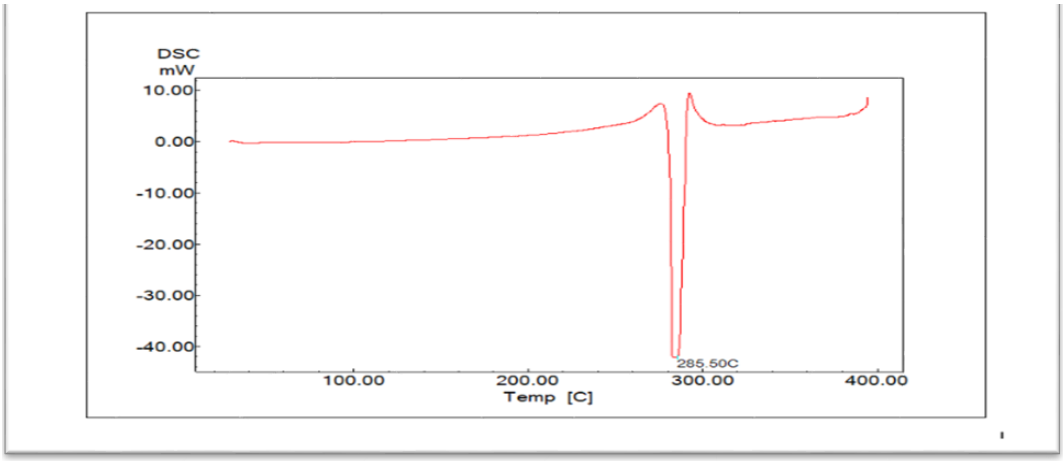

Fig. 2. Thermograms of Mesalazine.

Table 2. Animal groups and formula component.

groups	Rectal injection component
Gr1	Positively controlled (isopropyl alcohol)
Gr2	Negative control(phosphate buffer7.4)
Gr3	M11
Gr4	M11+sodium butyrate
Gr5	M11 in 1% hyaluronic acid
Gr6	M20
Gr7	M20+sodium butyrate
Gr8	M20 in 1% hyaluronic acid

different storage temperatures: 25 ± 2°C and 5 ± 2°C, for six months, and then the droplet size, PDI, and Uniformity of drug content were measured [50].

Statistical Analysis

Outcomes of the experiments, performed three times, were expressed as means and standard deviations (mean ± SD). To ascertain if there were any substantial differences between the groups in terms of their mean values, one-way analysis of variance (ANOVA) was used; p-values were considered significant at a threshold of ($P < 0.05$) and non-significant at ($p > 0.05$) [51].

RESULTS AND DISCUSSION

UV-wavelength (λmax) and Standard Curve

The lambda max of MSZ in ethanol was 331 nm, which is close to the value obtained by Rakesh Kumar Singh. [52] The phosphate buffer pH 7.4 was 330.5nm, which is close to the value in these references [41,42]. Calibration obtained in ethanol and phosphate buffer pH 7.4, and a standard curve was obtained, which has linear regression with R2

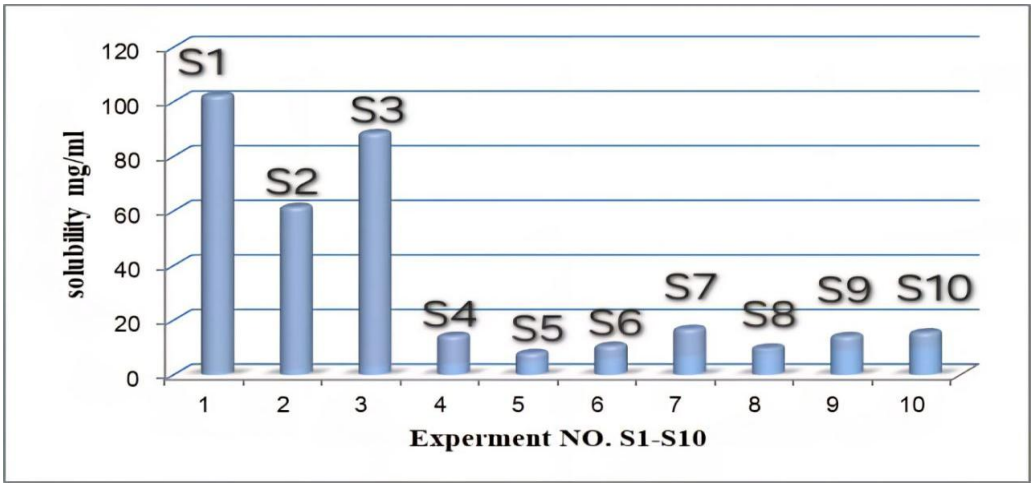

Fig. 3. Chart of solubility results of MSZ in various oils and surfactants

Table 3. Solubility of MSZ in different oils, surfactants, and

Experiments no.	media	Solubility	Color change
S1	Cremophor	101.24 ±0.023	Yes
S2	Propylene glycol	59.4 ±0.04	yes
S3	Vitamin E	85.5 ±0.041	No
S4	Imwitor308308	10.25 ±0.044	yes
S5	Jojoba oil	2.92 ±0.009	No
S6	Frankincense oil	4.59 ±0.018	no
S7	Grape oil	9.78 ±0.0023	No
S8	Sesame oil	1.84 ±0.011	No
S9	Clove oil	5.12 ±0.005	No
S10	Olive oil	5.47 ±0.017	No
S11	Labrafil oil	27.2 ±0.026	Yes
S12	Labrafac oil	4.5 ±0.0056	Yes

value equal to 0.9994 for the ethanol standard curve and a linear regression with R2 value equal to 0.997 in phosphate buffer pH 7.4.

Melting Point Determination

DSC provides the information on the physical characteristics of the sample. According to the thermograms Fig. 2, MSZ presented a sharp endothermic peak at 285.5°C, which agrees with references, *Gupta K, Roy SB, Newton AMJ, and Prabakaran* [53,54].

Solubility of MSZ in different oils, surfactants, and co-surfactants for nanoemulsion

The solubilization of MSZ in the oils was with a maximum concentration in Vitamin E (85.5 mg/ml) as illustrated in Table 3. Additionally, the solubility study in Cremophor and propylene glycol, a water-

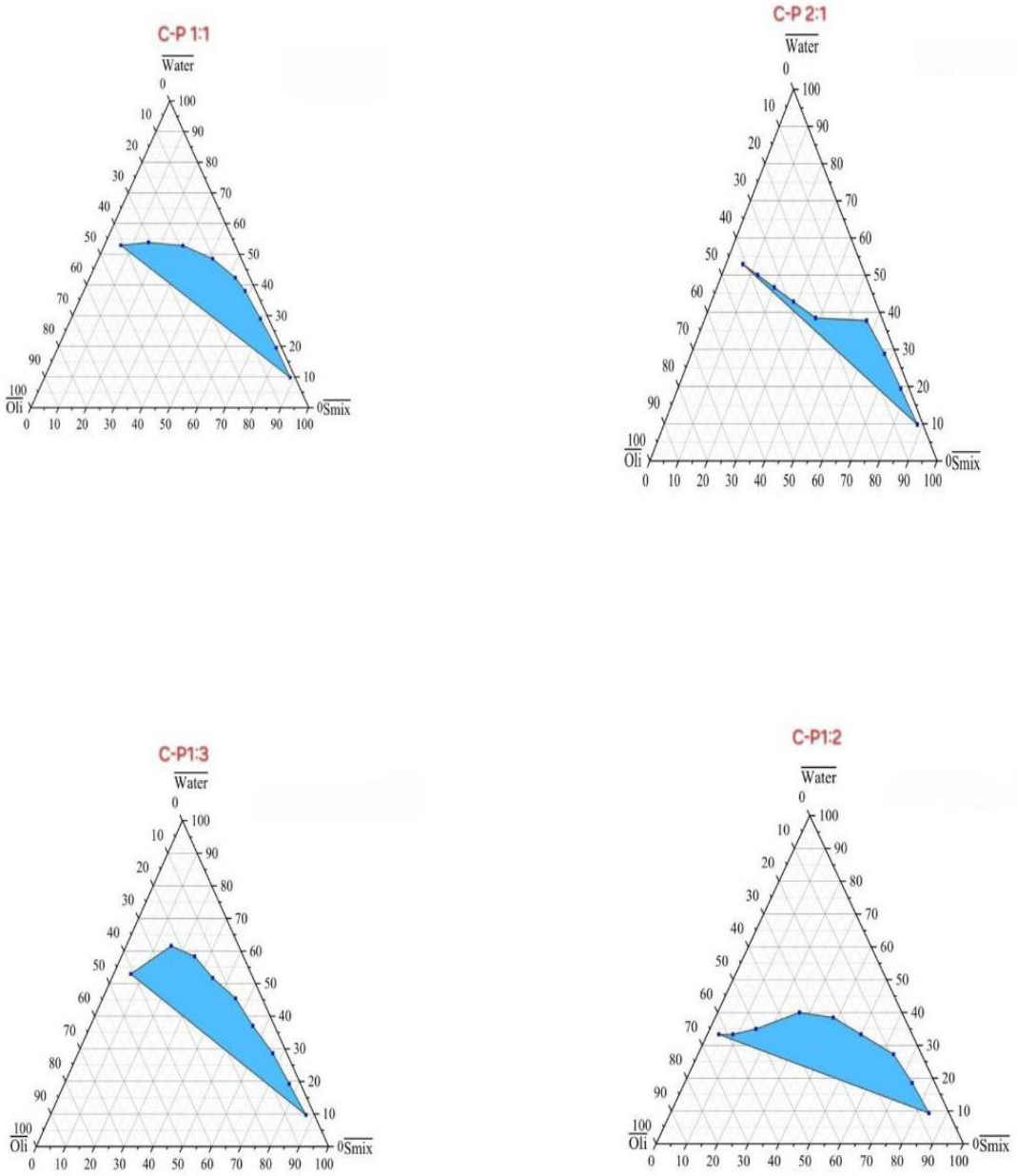

Fig. 4. Triangular coordinate oil-water emulsion diagram with

soluble non-ionic surfactant, shows a superior solubilizing concentration (101.24±0.023mg/ml). It has HLB =15which is an essential consideration for preparations.

The solubility of MSZ in surfactants and co-surfactants was measured, and the color change to deep brown was more significant in the case of using surfactants and co-surfactants than oils. The oxidation potentials enabled ranking the compounds by their susceptibility to oxidation. The color alteration of MSZ upon dissolution in surfactant and co-surfactant media occurred within less than 2 hours, indicating its susceptibility to oxidation. Theoretically, MSZ loses its aromaticity upon oxidation, transforming into a quinone. [55,56]. As in *E. S. Salih1; M. S. Al-Enizzi,* the investigation in their paper revealed that the blue dye product was generated exclusively in an alkaline medium; hence, the effects of several alkaline solutions (pH 9-12) and sodium hydroxide (pH > 12) were examined [57,54,59]

Cremophor and propylene glycol were mixed at constant weight ratios (1:1,1:2,1:3, and 2:1,3:1 w/w) to create the phase diagram. Figs.

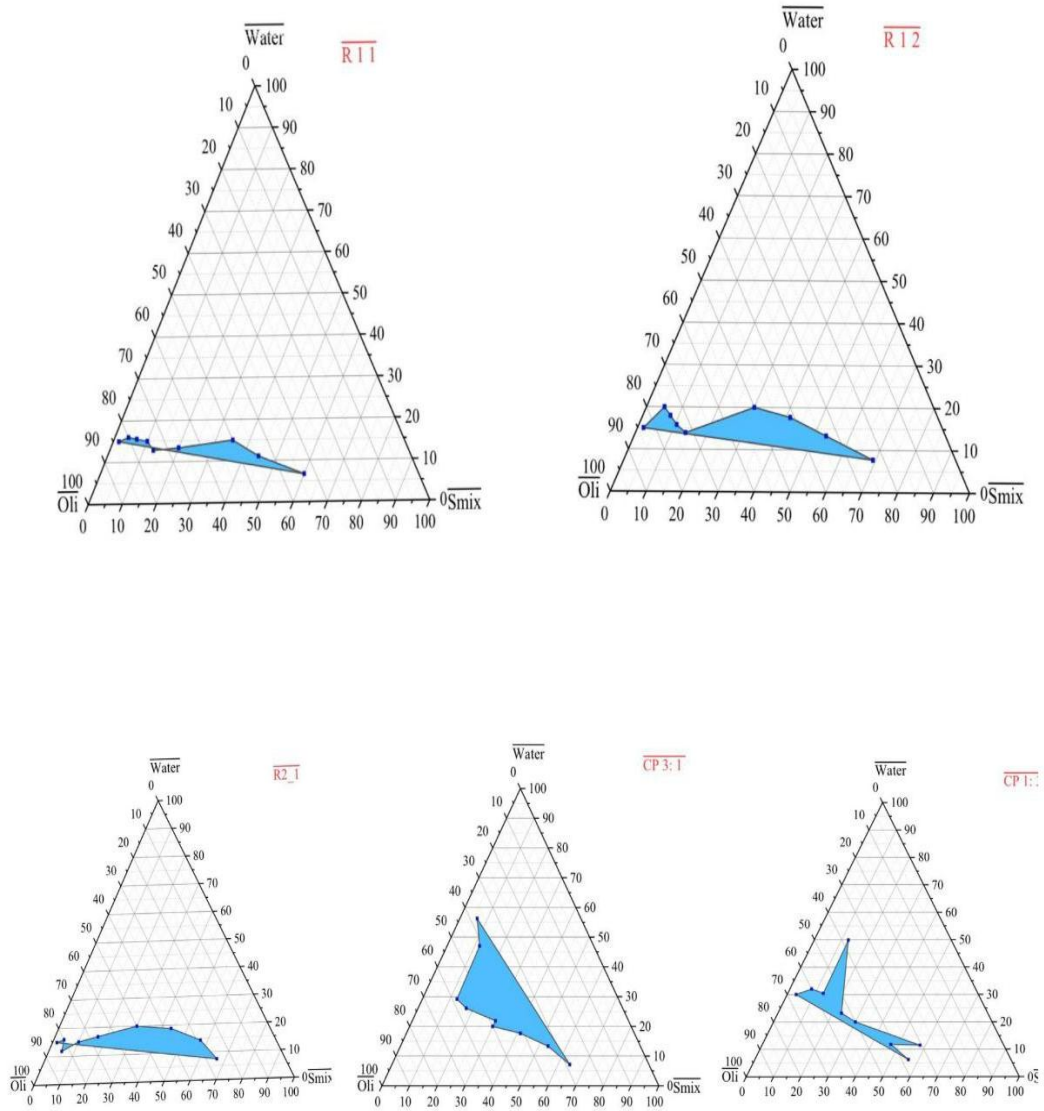

Fig. 5. Triangular coordinate oil-water emulsion diagram with different Smix (crimophore: propylene glycol) ratios e

4 and 5 include the resulting schematics made using different Smix; Cremophor and propylene glycol were combined in consistent weight ratios (1:1,1:2,1:3, and 2:1,3:1 w/w), subjected to an existence field of NS (the particular blue region). Typically, obtaining varied NS regions is the result of adjusting the Smix ratios. Furthermore, when the NS field size is big, which means the NS system is more efficient, the shaded portions represent the NE, and the unshaded zone represents the multiphase emulsion.

Thermodynamic Stability Studies

Investigation of Thermodynamic Stability Research on the thermodynamic stability of each manufactured NE formulation has been conducted. The findings in Table 4 indicate that the generated NEs exhibit phase separation and cracking, except for M11, M13, M14, M15, M16, M17, M18, M20, and M22, which showed good Thermodynamic Stability.

Nanoemulsion characterization

Droplet size measurement and polydispersity index (PDI)

Table 5 displays the formulated NE 'sPDI and droplet size average. The dimensions of the globules significantly influence the pace and amount of drug release from the formulation, absorption, and the stability of the nanoemulsion. Consequently, the assessment of nanoemulsion globule size is a crucial characteristic for evaluating its performance with the objective of formulation optimization. The quantity of Smix and the concentration of the dispersed phase have an impact on the NEs' droplet size. The prepared NE The formulations exhibited an average droplet size ranging from 6.7 nm to 574 nm. With the rise in Smix concentration, impact droplet sizes (M13 and M14) and (M15 and M16) decreased dramatically ($p<0.05$). The results suggested that a film forms surrounding the scattered globule. The emulsifier and co-emulsifiers form a complex

Table 4. Thermodynamic stability study results.

Formula code	H&C cycles	CEN. test	F-T cycles
M1	-	X	-
M2	-	X	-
M3	-	X	-
M4	-	X	-
M5	-	X	-
M6	-	X	-
M7	-	X	-
M8	-	X	-
M9	-	X	-
M10	-	X	-
M11	√	√	√
M12	X	X	X
M13	√	√	√
M14	√	√	√
M15	√	√	√
M16	√	√	√
M17	√	√	√
M18	√	√	√
M19	X	X	X
M20	√	√	√
M21	X	X	X
M22	√	√	√

**Pass expressed as √, failed expressed as X, heating, and cooling termed (H&C), centrifugation termed as (CEN), and freeze-thaw termed as (F&T)*

layer in the oil-in-water interface. The emulsifier and co-emulsifiers form a complex layer at the oil-in-water interface. This resulted in a markedly decreased interfacial tension between oil and water. The mixed interfacial layer was designed to be fluid and dual in a two-dimensional dispersion pressure environment [60].

The increasing ratio of surfactant mix resulted in a reduction in particle size, as seen by M13, which exhibited the smallest droplet size of 6.7 nm. This phenomenon is attributed to the structure of the surfactants, which facilitates their adsorption at the interface of the mixture due to their lipophilic "tail" and hydrophilic "head." Two categories of surfactants may be identified: primary and secondary. The principal surfactants are those whose characteristics enable the stabilisation of emulsions without the need to

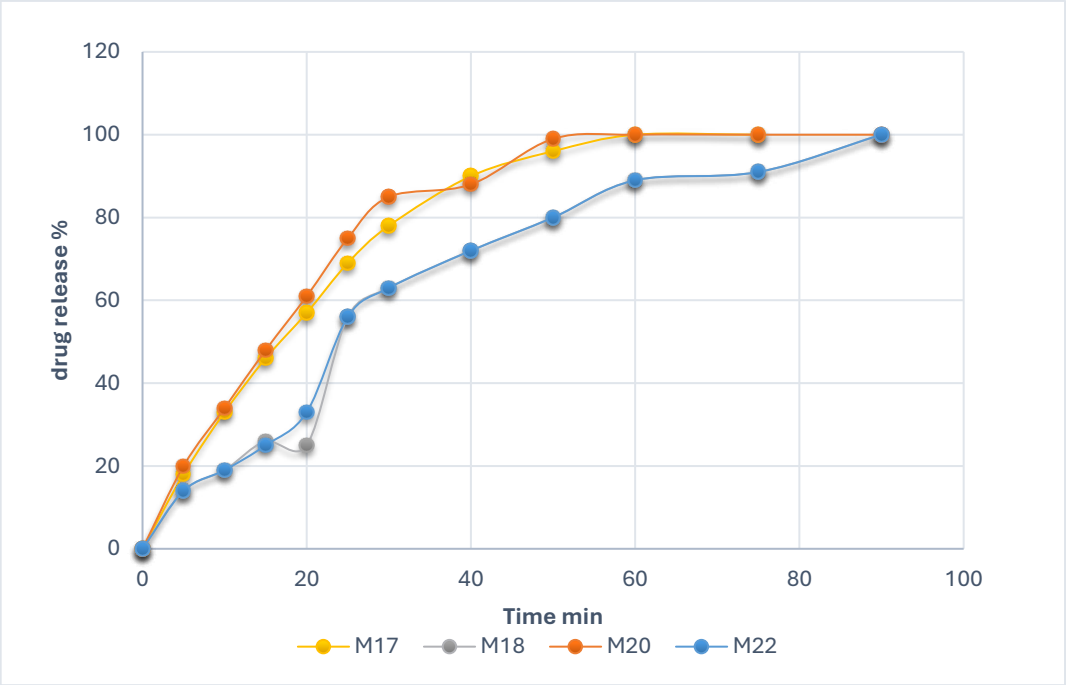

Fig. 7. Release of MSZ From Nanoemulsion Imwitor308.

Table 5 .PS, PDI, and Drug Content of Successfully Formed MSZ Nanoemulsion.

Formula code	Cremophor: propylene glycol	Type of oil	PS	PDI	Light transmittance%	Drug content
M11	1:2	VitE25%+imwitor30875%	28.43	0.0944	98%	99.7
M13	2:1	VitE25%+imwitor30875%	6.7	0.215	97%	88.5
M14	2:1	VitE25%+imwitor30875%	21.33	0.17	99%	95
M15	3:1	VitE25%+imwitor30875%	9.17	0.335	99%	97
M16	3:1	VitE25%+imwitor30875%	21.6	0.14	98%	97
M17	1:1	Imwitor308	574	0.56	96%	93.15
M18	2:1	Imwitor308	252	0.709	97%	98.89
M20	1:2	Imwitor308	30.8	0.11	99%	99
M22	1:3	Imwitor308	45	0.11	98%	93

include additional components for this function. Secondary surfactants, or co-surfactants, possess both polar and nonpolar structures within the same molecule (amphiphilic properties) and enhance the thermodynamic stability of these systems [61].

The polydispersity index, sometimes known as the PDI, is a measure that represents the variety of available particle sizes. A PDI number that is close to zero indicates that the particle size distribution is generally uniform. In contrast, a value that is close to one indicates that the distribution is

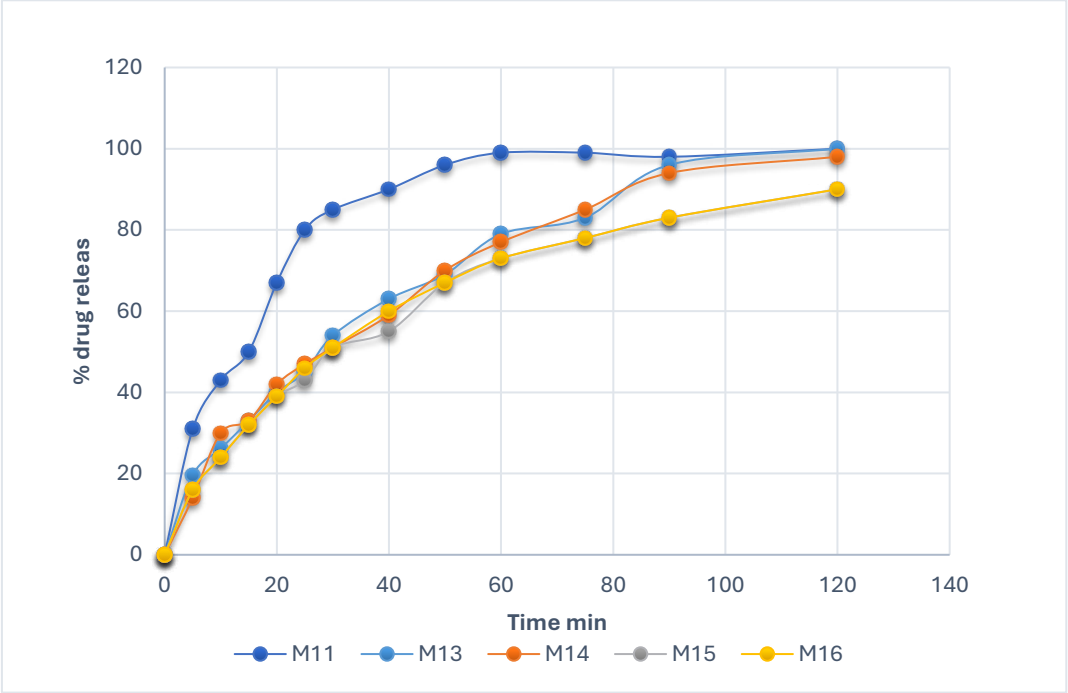

Fig. 6. Release of MSZ from nanoemulsion of VitE25%+imwitor30875%.

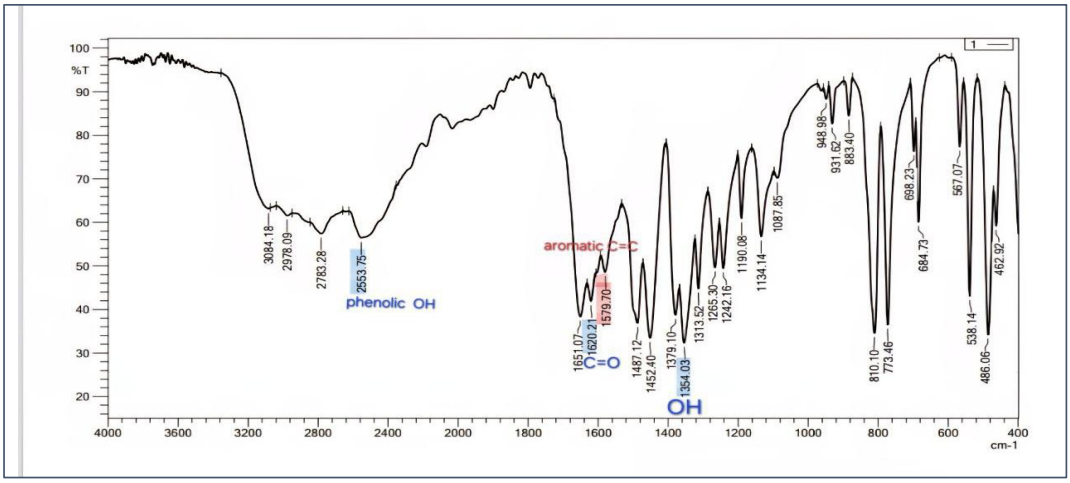

Fig. 8. Fourier transform infrared spectroscopy (FTIR) of pure MSZ.

substantially polydispersed within the particle size range. Given that the constructed formula had a PDI that was very close to zero (0,09-0.56), this indicates that the distribution was uniform.

Effect of type of oil on the prepared nanoemulsion and globule size

As shown in Table 4, the formula that uses vitamin E as the oil phase failed in thermodynamic stability. The stability of the said nanoemulsion was closely associated with the nano-droplets, which means the droplet size of (M1-M8) was larger than nano-scale, causing an increase in droplet size, thus increasing the tendency to undergo phase separation [62].

When we use a mixture of oil (Vitamin E25%+imwitor30875%), a stable nanoemulsion is formed as in M11, M13, M14, M15, and M16 with various particle sizes as shown in Table 5. M12 failed in thermodynamic stability because a low percentage of smix was used. In formulas, when we use imwitor308 as the oil phase in nanoemulsion preparation, the formula was successfully formed with the largest globule size, as shown in Table 5, in which M17 (574nm) and M18(252nm).

Effect of surfactant and co-surfactant ratio and percent of smix on prepared nanoemulsion and globule size

As shown in Table 5, M9 and M10 undergo phase separation with a surfactant and co-surfactant ratio of 1:1w/w (Cremophor: propylene glycol), even when they are done in a high percentage of smix, meaning the ratio is not enough to obtain

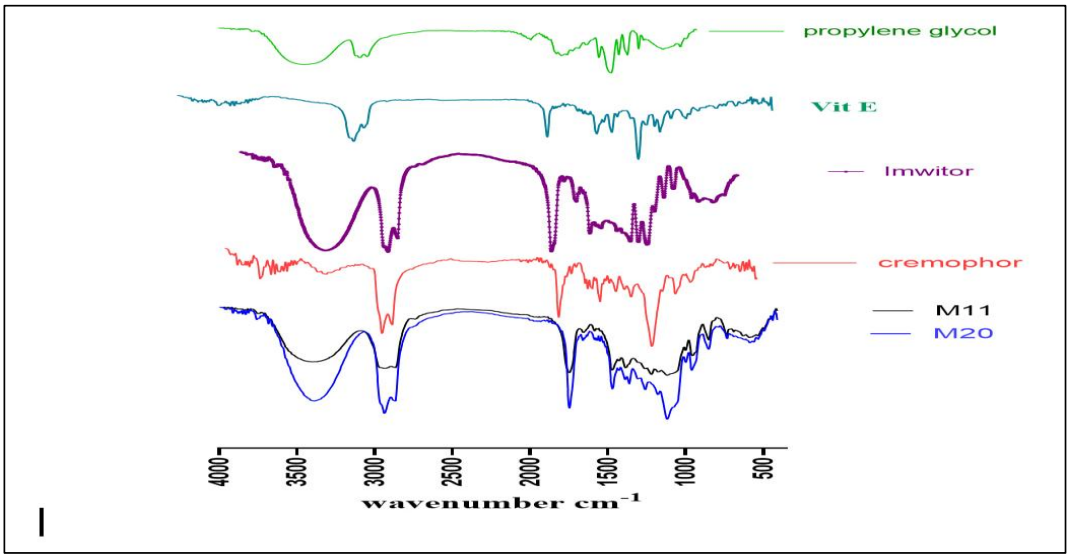

Fig. 9. Fourier transform infrared spectroscopy (FTIR) of nanoemulsion formula (M11 and M20) and formula component.

Table 6. Kinetic model of drug release.

Formula code	Zero order		First order		Higuchi	
	K_0	R_{seq}	K_1	R_{seq}	KH	R_{seq}
M11	1.102	0.6861	0.026	0.9867	9.587	0.9878
M13	1.089	0.6773	0.025	0.9886	9.485	0.9866
M14	1.004	0.6311	0.022	0.9867	8.778	0.9855
M15	1.011	0.6012	0.023	0.9878	8.865	0.9835
M16	1.307	-0.2088	0.058	0.9894	11.966	0.7857
M17	1.292	0.2117	0.047	0.9878	11.635	0.8722
M18	1.168	0.6835	0.029	0.9563	10.133	0.9140
M20	1.306	0.0930	0.051	0.9854	11.839	0.8393
M22	1.171	0.6703	0.030	0.9704	10.192	0.9276

nano-scale globules, which makes this formula fail in thermodynamic stability.

A stable nanoemulsion formula exhibits differences in globule size and PDI, influenced by varying S-mix component ratios and percentages during preparation. For example, in M11 (1:2 W/W ratio), the globule size is 28 nm. As the cremophor ratio increases, the particle size decreases to 6.7 nm at S-mix percentages of 55% and 60% respectively. Comparing M13 and M14, when the surfactant-to-co-surfactant ratio is 2:1 (W/W; Cremophor: propylene glycol), increasing the S-mix percentage leads to a decrease in globule size.

In vitro drug release

The purpose of the in-vitro release study was to check the drug release from the prepared formulas, as illustrated in the Figs. 6 and 7. The size of the droplets influences the quantitative release of the medicine from the NE formulation. The release profile of the formula that uses VitE25%+imwitor30875% as the oil phase is shown in Fig. 6. The release profile of the formula that uses imwitor308 as the oil phase is shown in Fig. 7. The f2 value shows a similar release profile of more than 50 for the formula prepared from VitE25%+imwitor30875%, except M11, which shows a dissimilar release profile with an f2 value

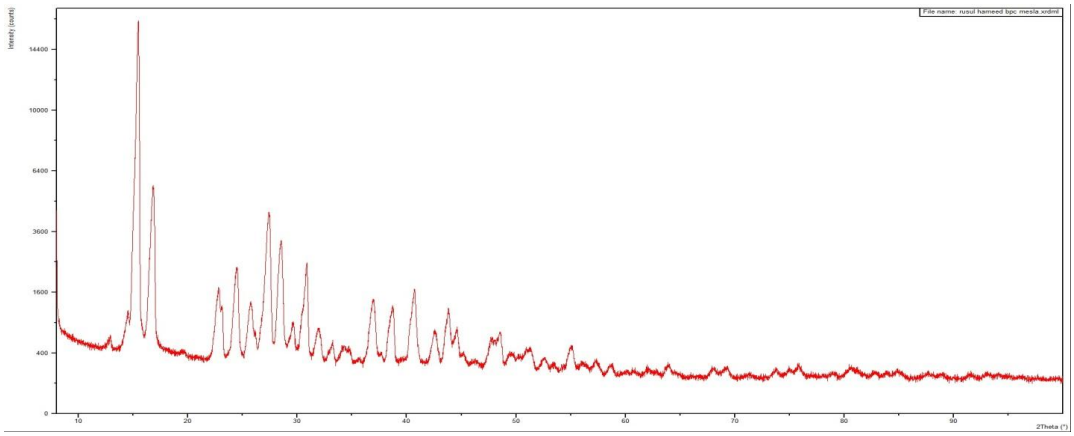

Fig. 10. PXRD of MSZ.

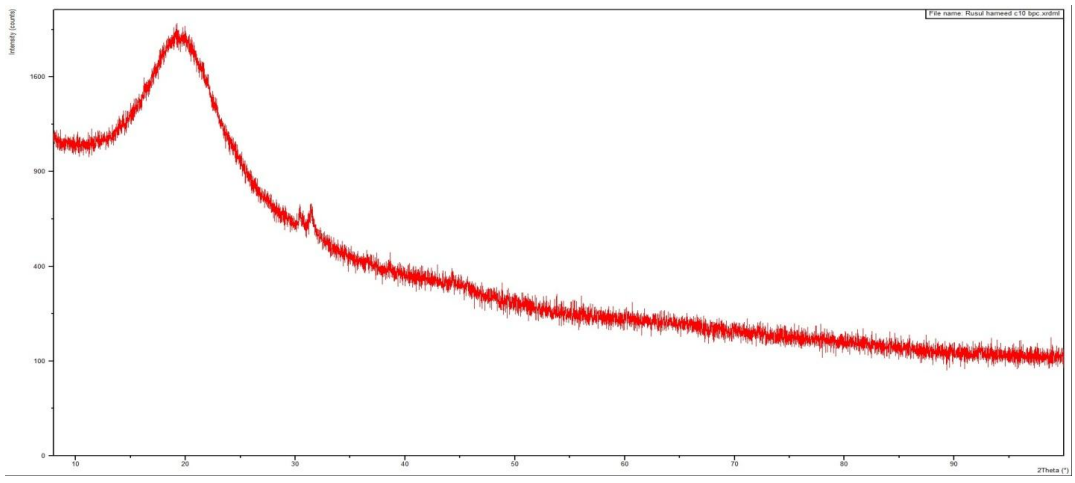

Fig. 11. PXRD of M11.

less than 50 when compared with other formulas.

For the formula prepared from Imwitor308 as the oil phase, the f2 value for M20 vs. M22 and M17 shows a dissimilar release profile with f2 less than 50, and when comparing M20 with M11, the f2 value is equal to 38, meaning the release profile of M11 is a better release profile.

The kinetic model of drug release, as shown in Table 6, depends on the R-squared value. The release kinetics are first order.

Fourier Transform Infrared spectroscopy (FTIR)

FT -IR spectrum of MSZ appears, with peaks at 1354 for (OH bending) Carboxylic acids and 1620 cm^{-1} for (C=O) Carboxylic acids, the peak at 2553 cm^{-1} for O-H stretching (phenolic and carboxylic that Intramolecular hydrogen bonds), the 1190 cm^{-1} and 773.46 cm^{-1} for (C -N), Primary amine (N-H bend) at 1651 cm^{-1}, the peak for C-H stretch of the aromatic group at 2978 cm, aliphatic stretching of C-H is allocated to 2783 cm^{-1}. Aromatic C=C peaks

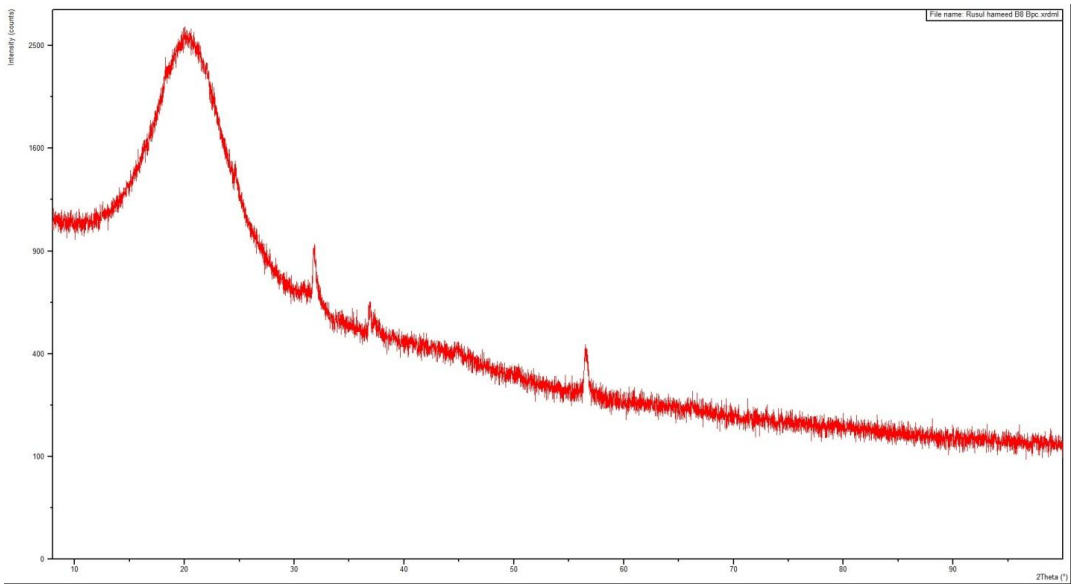

Fig. 12. PXRD of M20.

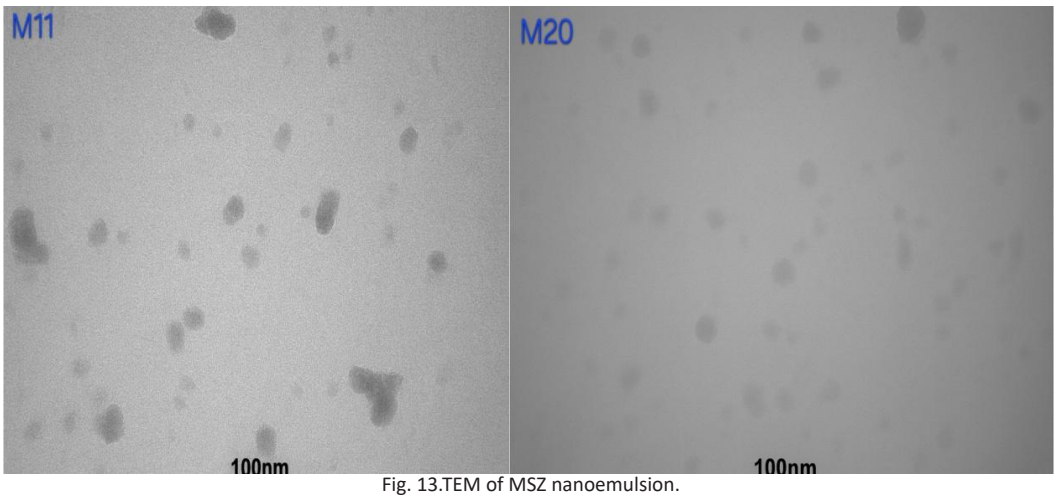

Fig. 13.TEM of MSZ nanoemulsion.

occur in the range 1579 cm^{-1}, which is consistent with references. [53,63,64]. The Cremophor spectra displayed distinct peaks at around 3502 cm^{-1} (indicative of OH stretching), 2923 cm^{-1} and 2855 cm^{-1} (representing C–H stretching), and 1730 cm^{-1} (related to C=O stretching) [65]. The ether C–O–C stretching manifested as a pronounced bandwidth at 1100 cm^{-1}, as seen in Fig. 9. The FTIR spectrum of vitamin E exhibited a distinctive C=O stretching vibration at around 900–1077 cm^{-1}, C–O formation at 1205 cm^{-1}, C=C formation at 1683 cm^{-1}, and C–H alkanes group at 2925 cm^{-1}. The absorption band of vitamin E at 3400–3650 cm^{-1} is ascribed to the terminal hydroxyl group, whereas the peak at 1050–1250 cm^{-1} is a result of C–O stretching [66].

Imwitor308 308 was characterized by a carbonyl ester peak at 1739 cm^{-1}, O–H stretching at 3388cm^{-1}, C–H stretching at 2926 and 2856 cm−1, and C–O stretching between 1000 and 1200

Fig. 14. Particle size of M11 and M20 after six months.

cm^{-1}, representing ester linkages that contribute to Imwitor308 emulsifying ability [67]. Propylene glycol shows the stretching vibration of the OH group at 3324 cm^{-1}. FTIR of M11 and M20 show vanish of the peak at 2553 cm^{-1} for O-H stretching (phenolic and carboxylic that Intermolecular hydrogen bonds) and appeared of new peak at this position, for M11(VitE25%+imwitor30875%) FTIR characteristic peak at 2918 cm^{-1} and 2856 cm^{-1} representing C–H stretching of Cremophor and 2731 cm^{-1} due to C-H starching of vitamin E, and 3360 cm^{-1} for Imwitor308 O–H stretching, that reveals now the MSZ in the inner layer [68], FTIR for M20(Imwitor308) the main peak is 2926 cm^{-1} and 2858 cm^{-1} representing C–H stretching of Cremophor, 3377 cm^{-1} for Imwitor308 O–H stretching.

Powder X-ray Diffraction (PXRD)

Distinct and pronounced peaks at around 15θ and 18θ were seen in the XRD pattern of mesalamine. Sharp and strong peaks at around 15θ and 18θ were found in the XRD pattern of mesalamine. Sharp and mighty peaks at around 15θ and 18θ were found in the XRD pattern of MSZ, PXRD of M11 and M20, producing a dome-shaped area. The pronounced and distinct peaks of the drug were absent in the XRD pattern of the drug-loaded nanoemulsion [68,69].

Morphological characteristics

TEM was used to perform the morphology of the optimized nanoemulsion formulation. From the TEM images of nanoemulsion (Fig. 13), it was observed that the Particles were uniformly distributed. Globules were spherical in shape with a size less than 100 nm, and they were discrete and non-aggregated.

Stability Assessment on Storage

The storage stability of the optimized MSZ nanoemulsion M11 and M20 was assessed over six months at two temperatures: 4°C (refrigerated) and 25°C. Particle size was evaluated with a Malvern Particle Size Analyzer, whilst encapsulation efficiency (EE%) was quantified spectrophotometrically at 330.5nm. A visual check was conducted to identify any precipitation of MSZ. The stability data show that the PS and PDI consistently remained low and within the nanoscale range (<100 nm) under all conditions, indicating that the nanoemulsion preserved its uniform size distribution and colloidal stability after six months of storage at both refrigerated

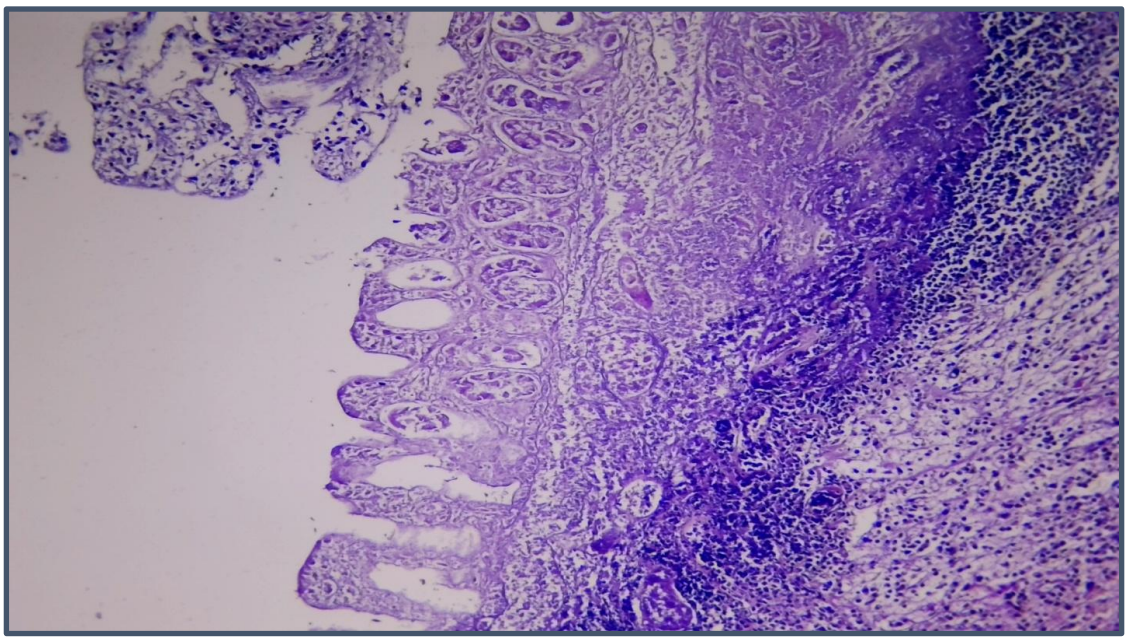

Fig. 15. Mucosal colonic section for positive control.

(4°C) and room temperature (25°C). The transparent appearance devoid of precipitation or turbidity further confirms the physical stability of the composition. The drug content results exhibited a little decline to 91% after six months at 25°C for M11 and 90% for M20, indicating minimal drug loss or degradation.

In vivo animal study

Animal description

Animals that are injected rectally with a formula containing sodium butyrate lose weight, and their

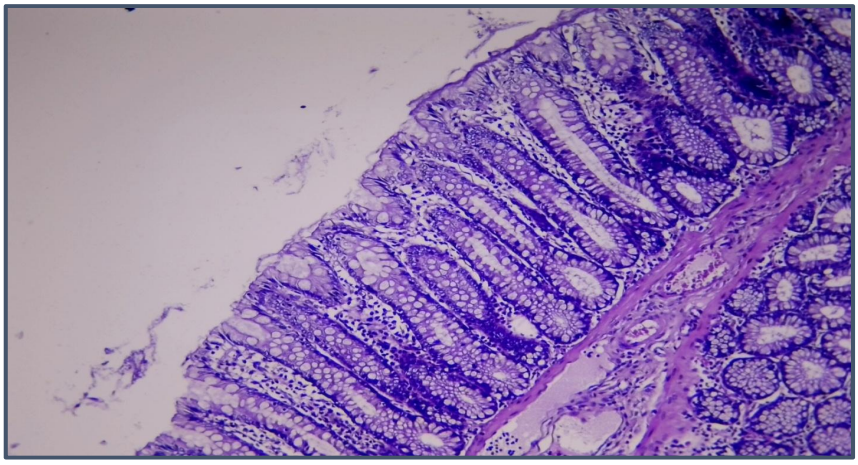

Fig. 16. Mucosal colonic section for negative control.

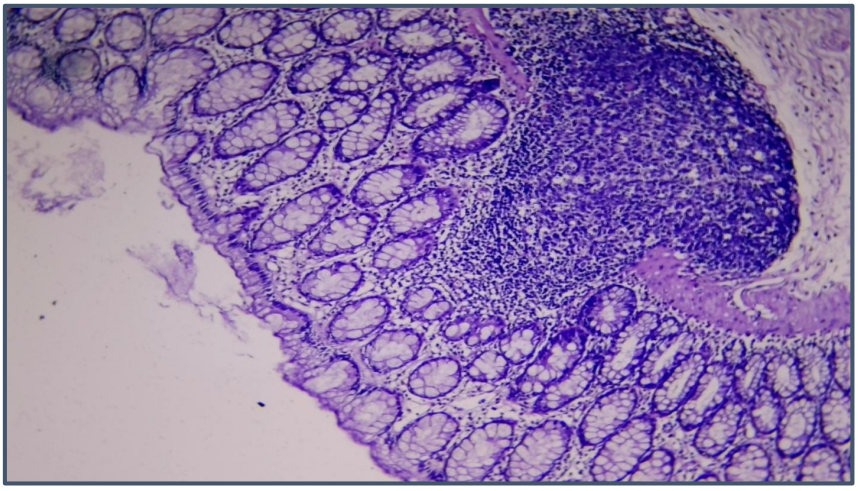

Fig. 17. Mucosal colonic section for a rat injected with M11.

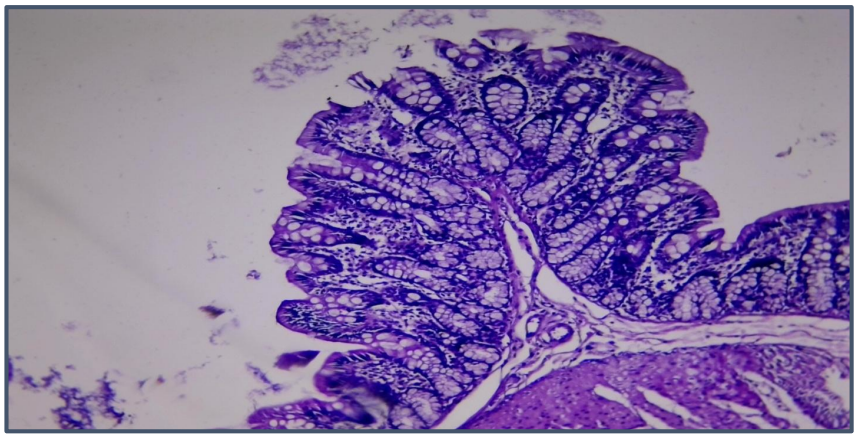

Fig. 18. Mucosal colonic section for a rat injected with M11in 1%hyaluronic acid.

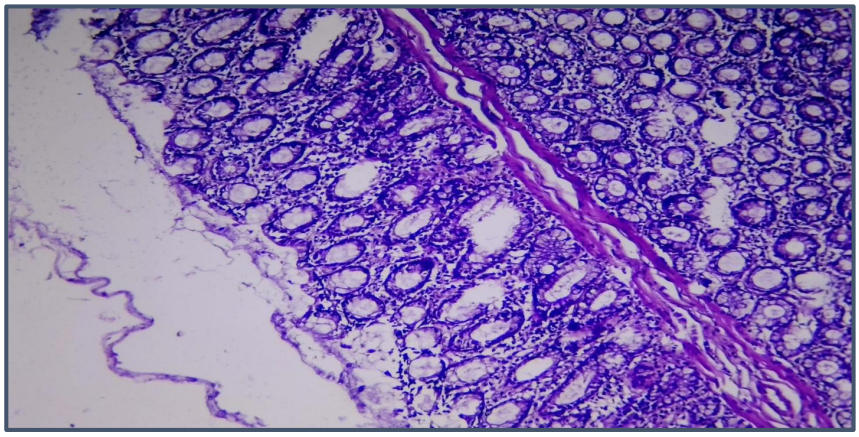

Fig. 19. Mucosal colonic section of a rat injected with M11 with sodium butyrate.

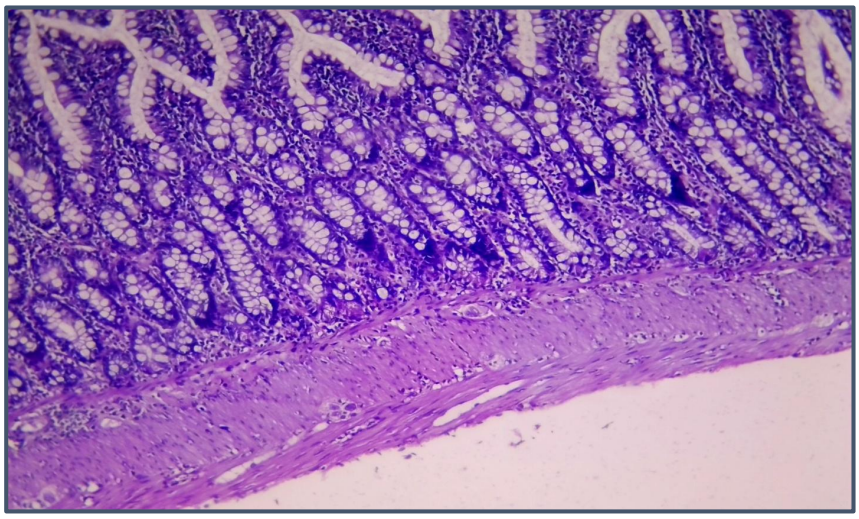

Fig. 20. Mucosal colonic section for a rat injected with M20e.

appetite decreases.

Histopathological examination of the colon

The colon section after one month is shown in Fig. 15, for the positive control, which shows irritation of the mucosa when compared to the negative control.

The animal group that administered M11 showed healthy colonic mucosa with the appearance of Peyer's patches, as shown in Fig. 17.

Peyer's patches are essential to mucosal immunity, significantly contributing to the Gut-associated lymphoid tissue. They are extensively dispersed throughout the small intestine, with the most significant density being in the human ileum, where they function as crucial antigen entry points for the immune system. Peyer's patches include 10–1000 individual follicles arranged into distinct lymphoid structures, which are covered by follicle-associated epithelium [70].

Fig. 18 shows a section of a rat injected with M11in 1% hyaluronic acid, which shows a healthy mucosal section, and Fig. 19 shows M11 with

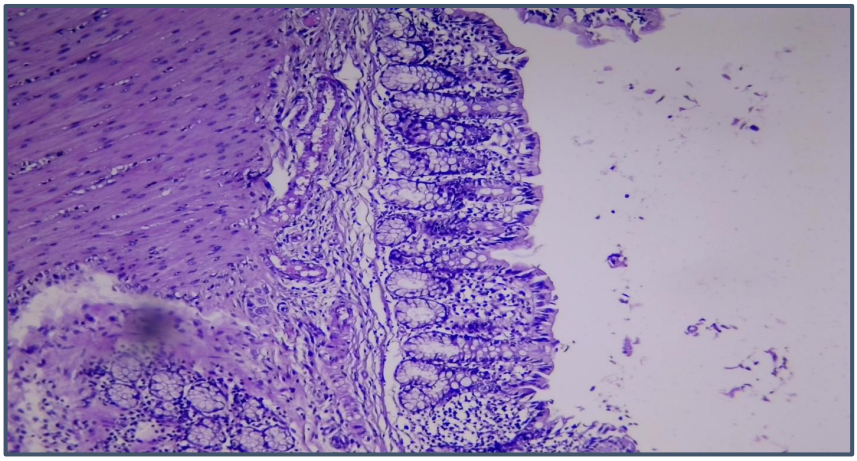

Fig. 21. Mucosal colonic section for a rat injected with M11 with sodium butyrate.

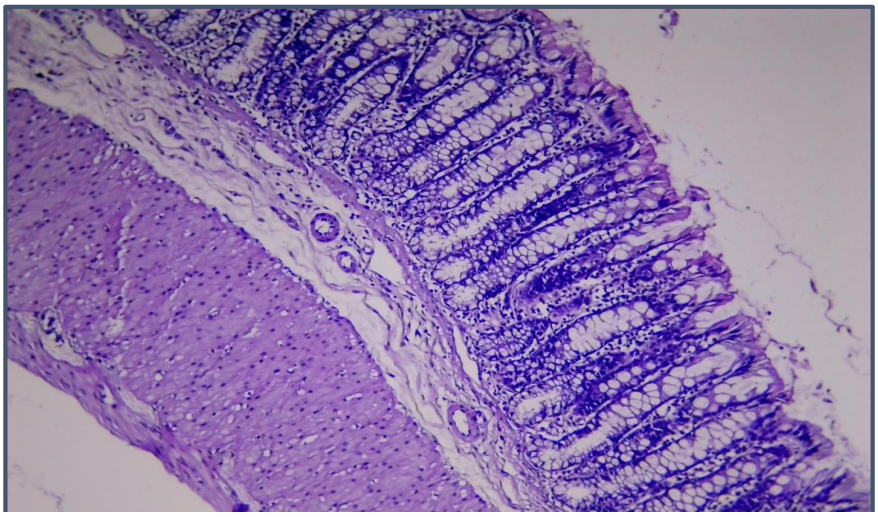

Fig. 22. Mucosal colonic section for a rat injected with M20in 1%hyaluronic acid.

sodium butyrate, in which the section shows an inflammatory cell.

Fig. 20 shows a mucosal rat section of a rat injected with the M20 formula, showing a healthy section. Fig. 21 for M20 with sodium butyrate, which shows the proliferation of inflammatory cells. Fig. 22 for the mucosa of a rat injected with M20 in 1%hyaluronic acid.

CONCLUSION

The study's findings suggest that MSZ was effectively transformed into a nanoemulsion, a novel method of drug delivery, which boosted intracolonic retention ($p<0.05$) and could potentially enhance its therapeutic effectiveness when administered intrarectally.

CONFLICT OF INTEREST

The authors declare that there is no conflict of interests regarding the publication of this manuscript.

REFERENCES

1. Arun Kumar MS, Rajesh M, Subramanian L. Solubility enhancement techniques: A comprehensive review. World Journal of Biology Pharmacy and Health Sciences. 2023;13(3):414-149.
2. Liu Y, Liang Y, Yuhong J, Xin P, Han JL, Du Y, et al. Advances in Nanotechnology for Enhancing the Solubility and Bioavailability of Poorly Soluble Drugs. Drug Des Devel Ther. 2024;Volume 18:1469-1495.
3. Samineni R, Chimakurthy J, Konidala S. Emerging Role of Biopharmaceutical Classification and Biopharmaceutical Drug Disposition System in Dosage form Development: A Systematic Review. Turkish Journal of Pharmaceutical Sciences. 2022;19(6):706-713.
4. Tarivitla LP, Reddy MS. An Overview of the Biopharmaceutics Classification System (BCS). GSC Biological and Pharmaceutical Sciences. 2021;14(2):217-221.
5. Khan AU, Khan M, Cho MH, Khan MM. Selected nanotechnologies and nanostructures for drug delivery, nanomedicine and cure. Bioprocess and Biosystems Engineering. 2020;43(8):1339-1357.
6. Gupta A, Eral HB, Hatton TA, Doyle PS. Nanoemulsions: formation, properties and applications. Soft Matter. 2016;12(11):2826-2841.
7. Nirmala MJ, Durai L, Gopakumar V, Nagarajan R. Preparation of Celery Essential Oil-Based Nanoemulsion by Ultrasonication and Evaluation of Its Potential Anticancer and Antibacterial Activity. International Journal of Nanomedicine. 2020;Volume 15:7651-7666.
8. Raine, June Munro, (born 20 June 1952), Director, Vigilance and Risk Management of Medicines Division (formerly Post Licensing Division), Medicines and Healthcare products Regulatory Agency, since 2003 (Director, Post-Licensing Division, Medicines Control Agency, 1998–2003), Department of Health. Who's Who: Oxford University Press; 2007.
9. Low energy methods for preparation of nanoemulsions and practical examples of nanoemulsions. Nanodispersions: De Gruyter; 2015. p. 217-238.
10. Aswathanarayan JB, Vittal RR. Nanoemulsions and Their Potential Applications in Food Industry. Frontiers in Sustainable Food Systems. 2019;3.
11. Prajapati BG, Parihar A, Macwan M, Pal S. A comprehensive review on applications, preparation and characterization of nanoemulsion. IP International Journal of Comprehensive and Advanced Pharmacology. 2023;8(2):104-111.
12. Zeng L, Xin X, Zhang Y. Development and characterization of promising Cremophor EL-stabilized o/w nanoemulsions containing short-chain alcohols as a cosurfactant. RSC Advances. 2017;7(32):19815-19827.
13. Liu Q, Huang H, Chen H, Lin J, Wang Q. Food-Grade Nanoemulsions: Preparation, Stability and Application in Encapsulation of Bioactive Compounds. Molecules. 2019;24(23):4242.
14. Widyaningrum I, Triyoga EF, Wibisono N, Kusumawati S, Widiyana AP. Type of Cosurfactant Effects on Particle Size in Nanoemulsion Drug Delivery Systems. East Asian Journal of Multidisciplinary Research. 2023;2(9):3811-3820.
15. Ripened Pu-erh Tea Extract Promotes Gut Microbiota Resilience against Dextran Sulfate Sodium Induced Colitis. American Chemical Society (ACS).
16. Wei H, Yu C, Zhang C, Ren Y, Guo L, Wang T, et al. Butyrate ameliorates chronic alcoholic central nervous damage by suppressing microglia-mediated neuroinflammation and modulating the microbiome-gut-brain axis. Biomedicine and Pharmacotherapy. 2023;160:114308.
17. Zhang Z, Zhang H, Chen T, Shi L, Wang D, Tang D. Regulatory role of short-chain fatty acids in inflammatory bowel disease. Cell Communication and Signaling. 2022;20(1).
18. BPC Papers. E-papers Servicos Editoriais Ltda; 2014. Report No.: 2357-7681.
19. Ahmed Elbashir A. Development and Validation of Spectrophotometric Methods for the Determination of Mesalazine in Pharmaceutical Formulation. Medicinal Chemistry. 2014;04(03).
20. Vaishnavi J, Pooja K, Kishor O, Mohini Y. Solubility Enhancement by Solid Dispersion Method: An Overview. Asian Journal of Pharmaceutical Research and Development. 2024;12(4):113-118.
21. Ye B. Mesalazine preparations for the treatment of ulcerative colitis: Are all created equal? World J Gastrointest Pharmacol Ther. 2015;6(4):137.
22. Aravindh Kumar SM, Rathakrishnan E. Rectangular tabs for elliptic jet control. 2015 International Conference on Fluid Power and Mechatronics (FPM); 2015/08: IEEE; 2015. p. 1399-1407.
23. Kassab HJ, Thomas LM, Jabir SA. Development and Physical Characterization of a Periodontal Bioadhesive Gel of Gatifloxacin. International Journal of Applied Pharmaceutics. 2017;9(3):31.
24. Al-Obaidi MSM, Al-Samarrai ET. Spectrophotometric determination of Mesalazine by a charge transfer complex. International journal of health sciences. 2022:10068-10078.
25. Güler E, Poturcu K, Rahimpour E, Jouyban A. Determination of the Mesalazine Solubility at Biorelevant Temperature. International Journal of Analytical Mass Spectrometry and Chromatography. 2024;12(01):1-12.
26. Jaafer H, Al-Kinani KK. Formulation and Evaluation of Idebenone Microemulsion as a Potential Approach for

the Transmucosal Drug Delivery Systems. Iraqi Journal of Pharmaceutical Sciences(P-ISSN 1683 - 3597 E-ISSN 2521 - 3512). 2024;33(1):79-88.
27. Preparation and Evaluation of Pharmaceutical Cocrystals for Solubility Enhancement of Ketoconazole. J Carcinog. 2025.
28. Okonogi S. Pseudoternary phase diagram construction v1. Springer Science and Business Media LLC; 2017.
29. Angela D, Carmen Z, Daniela Ş, MureŞAn EI, Gabriela L, Sinem Yaprak K, et al. Essential mint oil-based emulsions: preparation and characterization. Industria Textila. 2019;70(01):83-87.
30. Delmas T, Atrux-Tallau N, Goutayer M, Han SH, Kim JW, Bibette J. Nanoemulsions: Preparation, Stability and Application in Biosciences. Nanomaterials in Drug Delivery, Imaging, and Tissue Engineering: Wiley; 2013. p. 1-58.
31. Sadeq ZA. Review on Nanoemulsion: Preparation and Evaluation. International Journal of Drug Delivery Technology. 2020;10(01):187-189.
32. Solubility and dissolution enhancement of velpatasvir by nanoemulsion based gel formulation; preparation and in-vitro characterization. Interciencia. 2024.
33. Abbas IK, Shaimaa Nazar A-A. Design, Optimization and Characterization of Self-Nanoemulsifying Drug Delivery Systems of Bilastine. Iraqi Journal of Pharmaceutical Sciences(P-ISSN 1683 - 3597 E-ISSN 2521 - 3512). 2023;32(Suppl.):164-176.
34. B. Hamed S, N. Abd Alhammid S. Formulation and Characterization of Felodipine as an Oral Nanoemulsions. Iraqi Journal of Pharmaceutical Sciences (P-ISSN: 1683 - 3597 , E-ISSN : 2521 - 3512). 2021;30(1):209-217.
35. Al wiswasi N, Fatima JA-G. Brimonidine-Soluplus Nanomicelles: Preparation and in-vitro evaluation. Iraqi Journal of Pharmaceutical Sciences. 2025;34(1):246-255.
36. Amal Abdullah M, Shaimaa Nazar Abd A. Preparation, In Vitro Evaluation and Characterization studies of Clozapine Nanosuspension. Iraqi Journal of Pharmaceutical Sciences. 2025;33((4SI)):336-348.
37. Abdullah TM, Al-Kinani KK. Topical Propranolol Hydrochloride Nanoemulsion: A Promising Approach Drug Delivery for Infantile Hemangiomas. Iraqi Journal of Pharmaceutical Sciences(P-ISSN 1683 - 3597 E-ISSN 2521 - 3512). 2023;32(Suppl.):300-315.
38. Hammodi ID, N. Abd Alhammid S. Preparation and Characterization of Topical Letrozole Nanoemulsion for Breast Cancer. Iraqi Journal of Pharmaceutical Sciences (P-ISSN: 1683 - 3597 , E-ISSN : 2521 - 3512). 2020;29(1):195-206.
39. Sara Abdullah C, Nidhal Khazaal M. Preparation and Evaluation of Pimecrolimus Nanoemulsion for Topical Delivery. Iraqi Journal of Pharmaceutical Sciences. 2025;34(3):131-141.
40. N. Taher M, A.Hussein A. Formulation and Evaluation of Domperidone Nanoemulsions for Oral Rout. Iraqi Journal of Pharmaceutical Sciences (P-ISSN: 1683 - 3597 , E-ISSN : 2521 - 3512). 2017;24(2):77-90.
41. Nizar Awish J, Shaimaa Nazar Abd A. Formulation and Evaluation of Canagliflozin Self-nanomicellizing Solid Dispersion Based on Rebaudioside A for Dissolution and Solubility Improvement. Iraqi Journal of Pharmaceutical Sciences. 2025;33((4SI)):43-56.
42. Flekka K, Dimaki VD, Mourelatou E, Avgoustakis K, Lamari FN, Hatziantoniou S. Stability and Retention of Nanoemulsion Formulations Incorporating Lavender Essential Oil. Cosmetics. 2024;11(3):65.
43. Hashim HH, Jaber SA. Nanomicellar Dispersion-Based Approach to Improve Amisulpride Dissolution: Formulation, Characterization, and In Vitro Release Study. International Journal of Applied Pharmaceutics. 2025:181-192.
44. Thamer AK, Abood AN. Preparation and In vitro Characterization of Aceclofenac Nanosuspension (ACNS) for Enhancement of Percutaneous Absorption using Hydrogel Dosage Form. Iraqi Journal of Pharmaceutical Sciences (P-ISSN: 1683 - 3597 , E-ISSN : 2521 - 3512). 2021;30(2):86-98.
45. Salih OS, Hamoddi ZM, Taher SS. Development and Characterization of Controlled Release Tablets of Candesartan Cilexetil/ β-Cyclodextrin Inclusion Complex. International Journal of Drug Delivery Technology. 2020;10(02):273-283.
46. Salih OS, Nief RA. Effect of Natural and Synthetic Polymers on the Properties of Candesartan Cilexetil Matrix Tablet Prepared by Dry Granulation. Asian Journal of Pharmaceutical and Clinical Research. 2016;9(9):161.
47. Sulaiman HT, Jaber SH. Effect of Formulation Parameter on Dissolution Rate of Flurbiprofen Using Liquisolid Compact. Journal of Pharmaceutical Research International. 2021:289-306.
48. Abbas Ik, A. Rajab N, A. Hussein A. Formulation and In-Vitro Evaluation of Darifenacin Hydrobromide as Buccal Films. Iraqi Journal of Pharmaceutical Sciences (P-ISSN: 1683 - 3597 , E-ISSN : 2521 - 3512). 2019;28(2):83-94.
49. Laxmi M, Bhardwaj A, Mehta S, Mehta A. Development and characterization of nanoemulsion as carrier for the enhancement of bioavailability of artemether. Artificial Cells, Nanomedicine, and Biotechnology. 2014;43(5):334-344.
50. Bernardi DS, Pereira TA, Maciel NR, Bortoloto J, Viera GS, Oliveira GC, et al. Formation and stability of oil-in-water nanoemulsions containing rice bran oil: in vitro and in vivo assessments. Journal of Nanobiotechnology. 2011;9(1):44.
51. Maryam HA, Nidhal Khazaal M. Effect of Pluronic F127 Concentration on Gelling Temperature and other Parameters of Lomustine Mucoadhesive In-Situ Gel. Iraqi Journal of Pharmaceutical Sciences(P-ISSN 1683 - 3597 E-ISSN 2521 - 3512). 2024;33(3):63-71.
52. Ghurghure S, Sawant K, Deokar SS. UV Spectrophotometric Method Development and Validation of Mesalazine in Bulk and Solid Dosage Form (Research Article). International Journal of Pharmacy and Biological Sciences. 2021;11(1):131-135.
53. Sharma M, Joshi B, Bansal M, Goswami M. Formulation and Evaluation of Colon Targeted Tablets of Mesalazine. Journal of Drug Delivery and Therapeutics. 2012;2(5).
54. Saba Abdulhadi J, Nawal Ayash R. Preparation and In vitro/Ex vivo Evaluation of Nanoemulsion-Based in Situ Gel for Intranasal Delivery of Lasmiditan. Iraqi Journal of Pharmaceutical Sciences(P-ISSN 1683 - 3597 E-ISSN 2521 - 3512). 2024;33(3):128-141.
55. T. Aziz A, H. Sultan S. Spectrophotometric Determination of Mesalazine in Pharmaceutical Preparations by Oxidative Coupling Reactions with m-Aminophenol and 2,6- Dihydroxybenzoic Acid. Baghdad Science Journal. 2019;16(4).
56. Northern Branch. Public Health. 1942;56:49.
57. Elham SS, Mohammed A-E. Spectrophotometric Assay of

Mesalazine in Pharmaceutical Preparations Via Oxidative coupling reaction with o-cresol and sodium metaperiodate. Journal of Education and Science. 2020;29(1):279-292.
58. El Zein R, Ispas-Szabo P, Jafari M, Siaj M, Mateescu MA. Oxidation of Mesalamine under Phenoloxidase- or Peroxidase-like Enzyme Catalysis. Molecules. 2023;28(24):8105.
59. Dung NT, Dao DT, Hoat GD, Son NA. Development of Spectrophotometric Method for Determination of Ceftazidime with the Bratton–Marshall Reagent in Pharmaceutical Preparation. Vietnam Journal of Science and Technology. 2017;55(2):220.
60. Preeti, Sambhakar S, Malik R, Bhatia S, Al Harrasi A, Rani C, et al. Nanoemulsion: An Emerging Novel Technology for Improving the Bioavailability of Drugs. Scientifica. 2023;2023:1-25.
61. Souto EB, Cano A, Martins-Gomes C, Coutinho TE, Zielińska A, Silva AM. Microemulsions and Nanoemulsions in Skin Drug Delivery. Bioengineering. 2022;9(4):158.
62. Romes NB, Abdul Wahab R, Abdul Hamid M, Oyewusi HA, Huda N, Kobun R. Thermodynamic stability, in-vitro permeability, and in-silico molecular modeling of the optimal Elaeis guineensis leaves extract water-in-oil nanoemulsion. Sci Rep. 2021;11(1).
63. Hurst WJ, Toomey PB. Determination of Aflatoxins in Peanut Products Using Reverse Phase HPLC. J Chromatogr Sci. 1978;16(8):372-376.
64. Alam MM, Tasneem F, Kabir AKL, Rouf ASS. Study of Drug-Drug and Drug-Food Interactions of Mesalazine Through FTIR and DSC. Dhaka University Journal of Pharmaceutical Sciences. 2019;18(2):257-269.
65. Kraisit P, Hirun N, Limpamanoch P, Sawaengsuk Y, Janchoochai N, Manasaksirikul O, et al. Effect of Cremophor RH40, Hydroxypropyl Methylcellulose, and Mixing Speed on Physicochemical Properties of Films Containing Nanostructured Lipid Carriers Loaded with Furosemide Using the Box–Behnken Design. Polymers. 2024;16(11):1605.
66. Fathi M, Nasrabadi MN, Varshosaz J. Characteristics of vitamin E-loaded nanofibres from dextran. Int J Food Prop. 2017;20(11):2665-2674.
67. Abduljaleel ZZ, Al-Kinani KK. Formulation of Self-Emulsifying Microemulsion for Acemetacin Using D-Optimal Design: Enteric-Coated Capsule for Targeted Intestinal Release and Bioavailability Enhancement. Pharmaceutics. 2025;17(10):1270.
68. Silva HD, Cerqueira MA, Donsì F, Pinheiro AC, Ferrari G, Vicente AA. Development and Characterization of Lipid-Based Nanosystems: Effect of Interfacial Composition on Nanoemulsion Behavior. Food and Bioprocess Technology. 2019;13(1):67-87.
69. Chaisri W, Hennink W, Okonogi S. Preparation and Characterization of Cephalexin Loaded PLGA Microspheres. Curr Drug Del. 2009;6(1):69-75.
70. Ishii H, Isomoto H, Shikuwa S, Hayashi T, Inoue N, Yamaguchi N, et al. Peyer's Patches in the Terminal Ileum in Ulcerative Colitis: Magnifying Endoscopic Findings. J Clin Biochem Nutr. 2010;46(2):111-118.